THE ASTROPHYSICAL JOURNAL, 497:L105–L108, 1998 April 20

THERMAL WATER VAPOR EMISSION FROM SHOCKED REGIONS IN ORION[1]

MARTIN HARWIT,[2] DAVID A. NEUFELD,[3] GARY J. MELNICK,[4] AND MICHAEL J. KAUFMAN[5]
Received 1998 January 26; accepted 1998 February 20; published 1998 March 31

ABSTRACT

Using the Long Wavelength Spectrometer on board the *Infrared Space Observatory*, we have observed thermal water vapor emission from a roughly circular field of view approximately 75″ in diameter centered on the Orion BN-KL region. The Fabry-Perot line strengths, line widths, and spectral line shifts observed in eight transitions between 71 and 125 μm show good agreement with models of thermal emission arising from a molecular cloud subjected to a magnetohydrodynamic C-type shock. Both the breadth and the relative strengths of the observed lines argue for emission from a shock rather than from warm quiescent gas in the Orion core. Although one of the eight transitions appears anomalously strong and may be subject to the effects of radiative pumping, the other seven indicate an H_2O/H_2 abundance ratio on the order of 5×10^{-4} and a corresponding gas-phase oxygen-to-hydrogen abundance ratio on the order of 4×10^{-4}. Given current estimates of the interstellar, gas-phase, oxygen and carbon abundances in the solar vicinity, this value is consistent with theoretical shock models that predict the conversion into water of all the gas-phase oxygen that is not bound as CO. The overall cooling provided by rotational transitions of H_2O in this region appears to be comparable to the cooling through rotational lines of CO but is an order of magnitude lower than cooling through H_2 emission. However, the model that best fits our observations shows cooling by H_2O and CO dominant in that portion of the postshock region where temperatures are below ~800 K and neither vibrational nor rotational radiative cooling by H_2 is appreciable.

Subject headings: infrared: ISM: lines and bands — ISM: abundances — ISM: individual (Orion) — ISM: molecules — molecular processes

1. INTRODUCTION

The molecular hydrogen shock in the Orion BN-KL region has been studied intensively since the seminal work of Kwan & Scoville (1976) revealed emission from carbon monoxide with line widths on the order of 100 km s^{-1}. Following this, Beckwith et al. (1978) identified the ro-vibrational transitions of molecular hydrogen emanating from this same region. Somewhat later, Beck (1984) provided a map of the region in the [v = 0–0 $S(2)$] 12.3 μm line, while studies by Watson et al. (1980, 1985) and Stacey et al. (1983) identified highly excited far-infrared rotational transitions from CO involving rotational levels ranging from $J = 15$ up to $J = 34$. Watson (1982), Viscuso et al. (1985), and Melnick et al. (1990) also studied OH transitions, with a view to understanding the dynamics and chemistry of the shocked and postshock domains.

More recently, Sugai et al. (1994) have provided a detailed map of the molecular hydrogen emission. They mapped a $4' \times 4'$ region with a spatial resolving power of 5.″3 in the H_2 [v = 1–0 $S(1)$] transition and found substantial emission from an elongated patch roughly 2′ in length and 1.′5 wide. In this region, they resolved nine separate emission peaks in a structure whose outlines are roughly bipolar, straddling the central source IRc2. While many smaller peaks abound, the overall structure is generally interpreted in terms of a bipolar wind emanating from IRc2 and plowing into an ambient H_2 cloud.

Most theoretical studies of the Orion shocked region (Draine & Roberge 1982; Chernoff, Hollenbach, & McKee 1982; Neufeld & Melnick 1987) have concluded that a rich emission spectrum from thermally excited water vapor must be playing a significant role in cooling the gas. However, with few exceptions—such as observations of maser emission from extremely dense regions or observations of relatively low excitation lines of the isotopic molecules HDO and $H_2{}^{18}O$ (e.g., Zmuidzinas et al. 1995)—the direct detection of water vapor emission has not been possible. Although thermal water vapor emission, largely confined to the far-infrared, has long been sought, telluric water vapor is an efficient absorber in the mid- and far-infrared and blocks precisely those wavelengths at which interstellar shocks are expected to emit the bulk of their radiation. While Cernicharo et al. (1994) have reported detection of the 183.3 GHz radio frequency 3(1, 3)–2(2, 0) transition, decisive observations had to await the launch of mid- and far-infrared spectral instrumentation into space. The *Infrared Space Observatory* (*ISO*), placed into Earth orbit in 1995 November, has provided a first opportunity to study these shocks systematically. Here we provide evidence that this emission has now been reliably observed.

2. OBSERVATIONS

On 1997 October 6, we observed the Orion BN-KL region with *ISO* (cf. Kessler et al. 1996) from 06:02:47 to 07:58:05 UT for a total of 6918 s. All observations were made in the Long Wavelength Spectrometer's Fabry-Perot (LWS/FP) mode (Clegg et al. 1996). The instrument's roughly circular field of view was centered on the epoch 2000 coordinates $5^h35^m14.^s2$, $-5°22'23.''3$.

We obtained data on eight H_2O lines. These detections required the use of four different detectors, each having its own roughly elliptical beam size: $70'' \times 68''$ at 125 and 121 μm, $77'' \times 71''$ at 99.5, 95.6, and 90 μm, $82'' \times 76''$ at 83 and 82

[1] Based on observations with the *Infrared Space Observatory*, an ESA project with instruments funded by ESA Member States (especially the PI countries: France, Germany, the Netherlands, and the UK) with the participation of ISAS and NASA.

[2] 511 H Street SW, Washington, DC 20024-2725 (also Department of Astronomy, Cornell University).

[3] Department of Physics and Astronomy, Johns Hopkins University, Charles and 34th Street, Bloomberg Center, Baltimore, MD 21218.

[4] Harvard-Smithsonian Center for Astrophysics, 60 Garden Street, Cambridge, MA 02138.

[5] NASA Ames Research Center, MS 245-3, Moffett Field, CA 94035-1000.

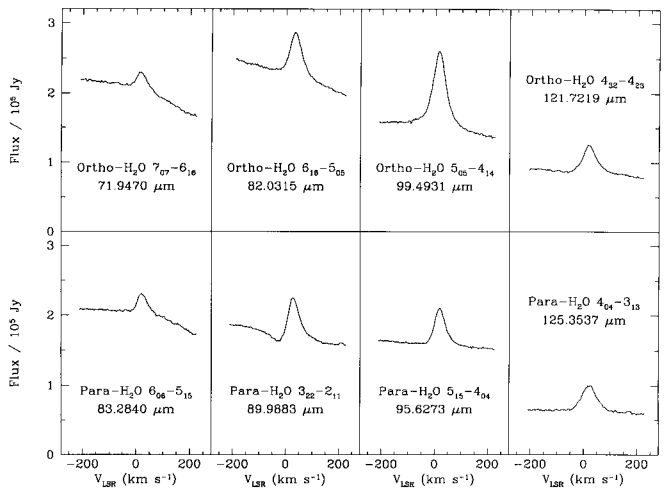

FIG. 1.—Line profiles of the observed transitions listed in Table 1. The error bars showing standard deviations from a mean obtained in successive spectral scans are too small to be discerned on this scale. The corrections, however, were made by eliminating grossly deviant data points resulting from cosmic-ray impacts on detectors. Given the large number of scans obtained, these subtractions did not significantly alter the final results.

μm, and $83'' \times 79''$ at 72 μm. The fields of view, therefore, differed by $\pm 19\%$.

In the wavelength range from 72 to 125 μm, the LWS/FP's spectral resolving power gradually increases from ~7000 to a peak of ~9800 at 95 μm, before slowly dropping to ~9500 at 125 μm. We repeatedly stepped the Fabry-Perot over a wavelength range that spanned 5 resolution elements on either side of each line. This made for a total of 11 resolution elements, each of which was sampled at eight equally spaced positions within the element, in what is designated as the "rapid scanning" mode of operation, each measurement lasting only 0.5 s. Strong signals were observed in all eight lines (see Fig. 1).

3. RESULTS

The main observational results are listed in Table 1. The first column identifies the transitions observed and indicates whether the line is emitted by ortho- or para-H_2O. The second column gives the wavelength. The third column lists the line-center displacement in terms of velocity with respect to the local standard of rest. Like all the other observational parameters listed in Table 1, this was determined from a Gaussian line fit. Since the spectral resolving power of the Fabry-Perot spectrometer ranges from 9000 to 7000, the lines necessarily are broader than 33–43 km s^{-1}. The relatively small spread of central line velocities observed, ± 8 km s^{-1}, probably is due to noise and suggests that all of the lines are emitted from one and the same region. Inspection of Figure 1, where the observed line profiles are displayed, visually confirms the quality of the data and shows the small statistical errors that arise in comparing the many scans taken over each of the lines. Column (4) of Table 1 gives the line widths. These widths are on the order of 60 km s^{-1} FWHM, significantly exceeding the minimum line width of 33–43 km s^{-1} determined by the spectral resolving power. They are consistent with an intrinsic line-of-sight velocity distribution that is Gaussian with FWHM ~ 35 km s^{-1}, convolved with the Fabry-Perot's Lorentzian profile at the above-stated resolving power. This estimate of the intrinsic line width is supported by additional observations toward Orion Peak 1 to be reported elsewhere. These made use of *ISO*'s Short Wavelength Spectrometer, whose resolving power of ~31,000 displayed a 42 km s^{-1} FWHM velocity distribution in the 4_{32}–3_{03} H_2O emission line at 40.69 μm.

Column (5) of Table 1 shows the total flux measured in each line. Columns (6) and (7) involve theoretical modeling and are discussed below. Column (8), the last column, provides the detected continuum level. It is substantial and underscores the importance of correct continuum subtraction. At 100 μm, a flux of $\sim 1.5 \times 10^5$ Jy corresponds to $\sim 5 \times 10^{-17}$ W cm^{-2} per resolution element, comparable to the total line flux.

The calibration of the LWS/FP is a complex procedure that continues to be refined. It consists, in the first place, of a calibration of the LWS detector response in the instrument's grating mode. This is periodically monitored through the use of five infrared illuminators incorporated into the instrument and by observing selected astronomical calibration sources. The response in the Fabry-Perot mode, for which the grating serves as an order sorter, is then deduced primarily from a preflight calibration of the Fabry-Perot etalon's added transmission losses.

As seen in the line plots of Figure 1, the continuum appears to be steep for some of the lines. A variety of factors contribute to these slopes. They include changes in the transmission function of the blocking filters and grating, a changing detector response function, and interference effects within the instrument that lead to sizable fringe amplitudes. To the extent that our continuum levels agree with continuum observations obtained by others, they nevertheless provide us with a means of ascertaining the reliability of the line fluxes we list.

Werner et al. (1976) mapped the same region of Orion we

TABLE 1

LWS LINES OBSERVED TOWARD ORION BN/KL

Line (1)	λ (μm) (2)	V_{LSR} (km s^{-1}) (3)	ΔV (km s^{-1}) (4)	Line Flux (W cm^{-2}) (5)	Line Flux/ KN-CMJS Prediction (6)	Inferred Abundance $n(H_2O)/n(H_2)$ (7)	Continuum Flux (Jy) (8)
4_{04}–3_{13} (para)	125.3537	21	70	2.2×10^{-17}	1.0	3.5×10^{-4}	6.2×10^4
4_{32}–4_{23} (ortho)	121.7219	27	65	2.2×10^{-17}	5.2	1.8×10^{-3}[a]	8.5×10^4
5_{05}–4_{14} (ortho)	99.4931	17	70	7.4×10^{-17}	1.4	4.9×10^{-4}	1.5×10^5
5_{15}–4_{04} (para)	95.6273	23	50	2.8×10^{-17}	1.5	5.3×10^{-4}	1.6×10^5
3_{22}–2_{11} (para)	89.9883	33	54	3.7×10^{-17}	1.85	6.5×10^{-4}	1.6×10^5
6_{06}–5_{15} (para)	83.2840	27	45	1.6×10^{-17}	1.3	4.6×10^{-4}	2.0×10^5
6_{16}–5_{05} (ortho)	82.0315	22	61	4.8×10^{-17}	1.2	4.2×10^{-4}	2.2×10^5
7_{07}–6_{16} (ortho)	71.9470	23	64	2.6×10^{-17}	1.1	3.8×10^{-4}	2.0×10^5

[a] This abundance estimate should be regarded as an upper limit, because the 121.7 μm line flux is significantly enhanced by radiative pumping, a process neglected in the KN model.

observed, with a field of view 1′ in diameter, and described its spectrum as a blackbody at 70 K with a 20 μm/λ emissivity beyond 20 μm. We find rough agreement in the spectral distribution of our continuum values with the spectral shape they describe. Moreover, the peak flux Werner et al. observed at 100 μm with a 40 μm bandwidth was 9×10^4 Jy. The continuum flux levels listed in Table 1 were all obtained with larger fields of view, but if we roughly prorate our observed flux to the smaller field of view of Werner et al., taking into account that their maps show a rapid decrease in flux away from the peak, we derive respective fluxes of ~0.64, ~1.25, and $\sim 1.57 \times 10^5$ Jy at 121.7, 99.49, and 82.03 μm. Since these three values provide a rough sampling of their wavelength range, we can average them to obtain a mean value of $\sim 1.15 \times 10^5$ Jy or 25% higher. Werner et al. estimated the uncertainties in their absolute flux levels at $\pm 20\%$. Summing the two uncertainties of 25% and 20% in quadrature, we obtain an uncertainty in the continuum fluxes listed in Table 1 of $\sim \pm 35\%$. On the basis of this comparison, we estimate our line fluxes to be similarly uncertain by $\sim \pm 35\%$. As the Long Wavelength Spectrometer characteristics become better established in the next few months, this error budget may be revised.

4. MODEL

The luminosity of water vapor emission from the Orion shock was predicted by Kaufman & Neufeld (1996, hereafter KN) and in Kaufman (1995). Their model solved for the equilibrium populations of the lowest 179 rotational levels of ortho-H_2O and for the lowest 170 rotational levels of para-H_2O. The model included cooling due to ro-vibrational transitions of H_2O, H_2, and CO and to dissociation of H_2. Cooling through gas-grain collisions was also included.

Water vapor in shocks is formed through reactions of atomic oxygen with molecular hydrogen to form OH radicals, which subsequently react with hydrogen molecules to form water vapor (Elitzur & de Jong 1973; Elitzur & Watson 1978). Once the shock-generated temperatures exceed ~400 K, the KN model predicts that all the oxygen not already incorporated in CO will be converted into H_2O. This is shown by computations that predict the relative abundances of the primary oxygen-bearing species, H_2O, OH, O, and O_2, throughout the shock. Expected spectral line emission from each of these species is computed using an escape probability formalism. The calculations included emission from the lowest 60 rotational states of ^{12}CO, as well as ^{13}CO, and the lowest 21 rotational states of H_2. For both molecular hydrogen and water vapor, the ortho/para ratio was assumed to be 3:1. Vibrational transitions from states up to $v = 2$ for CO and H_2 were included, as were ν_2 band transitions of H_2O.

In order for a shock not to dissociate interstellar molecules, the cloud through which it passes must be able to cool itself appreciably more quickly than it is heated by the shock. This will generally happen only if a magnetic field is present and precompresses the medium in what Draine (1980) has termed a continuous or "C-type" shock. This more gradual compression becomes possible because the Alfvén speed exceeds the speed of sound in the cloud. A magnetic precursor penetrates the cloud before the arrival of a J-type shock front in the wake of which temperatures and densities could sharply jump to dissociate the molecules.

KN considered a C-shock and predicted the H_2O emission from Orion by assuming the gas-phase oxygen and carbon abundances of Pollack et al. (1994), which were premised on solar system elemental abundances and a model of the shocked region in Orion based on data primarily obtained in CO and H_2 observations. These indicated a best fit for a shock velocity $v_s = 37$ km s^{-1} and a preshock H_2 density of 10^5 cm^{-3}. These values were constrained by the observed line-strength ratios of two pairs of spectral lines: the CO ($J = 34$–33) and ($J = 21$–20) lines and the H_2 [$v = 1$–0 $S(1)$] and [$v = 2$–1 $S(1)$] lines.

The shock velocity and hydrogen density do not depend on the assumed oxygen abundance, but the expected water vapor density does. Based on the work of Pollack et al. (1994), KN assumed the gas-phase abundances of oxygen and carbon nuclei to be, respectively, 5.45×10^{-4} and 1.2×10^{-4} relative to hydrogen nuclei. This led to the prediction that the water vapor abundance would be as high as $n(H_2O)/n(H_2) = 8.5 \times 10^{-4}$ and that the H_2, H_2O, and CO lines, respectively, should radiate away 75%, 21%, and 4% of the shock energy. More recent data by Cardelli et al. (1996, hereafter CMJS), however, indicate that the gas phase in diffuse interstellar clouds within 600 pc of the Sun exhibits a remarkably constant abundance of carbon and oxygen, with $n(O)/n(H) = 3.16 \times 10^{-4}$ and $n(C)/n(H) = 1.4 \times 10^{-4}$. In a preliminary calculation applied to Orion, we find that this substantially lower oxygen abundance predicts a correspondingly reduced water vapor concentration, $n(H_2O)/n(H_2) \sim 3.5 \times 10^{-4}$, and a drop in water vapor cooling that is close to proportional to the drop in abundance. The H_2:H_2O:CO cooling ratios thus become 88:8:4.

To determine the expected H_2O flux from Orion, we still need to know the value of a projection parameter that KN call Φ. It is the ratio of the actual surface area of the shock(s) to the projected area of the beam at the distance of the source. For a complex region, the field of view may contain n shocks, and the function Φ is summed over all of them. For a beam-filling planar shock, $\Phi = 1$; for a beam-filling spherical shock, $\Phi = 4$.

Observationally, the value of Φ is derived as the ratio of the radiant energy observed to the mechanical inflow energy expected for a beam-filling planar shock seen face-on. For the Orion shock, we infer the value of Φ from an estimate of the total surface brightness in our 75″ field of view, summed over all H_2 emission lines. To this end, we use Beck's (1984) H_2 [$v = 0$–0 $S(2)$] intensity averaged over the observed field of view as a tracer for the total H_2 emission—much of which is not directly observable because it is extinguished by ambient dust. Beck's data averaged over our field of view give a 12.3 μm intensity of $\sim 1.6 \times 10^{-3}$ ergs cm^{-2} s^{-1} sr^{-1}, when corrected by a factor of ~2 for 0.75 mag of extinction. The KN model indicates that the 12.3 μm flux needs to be multiplied by a factor of ~530, under the assumed density and shock velocity conditions, to yield a total intensity summed over all H_2 spectral lines. Although this multiplier is large, we have confidence that it is quite accurate and that it reliably implies a total H_2 intensity of ~0.85 ergs cm^{-2} s^{-1} sr^{-1}. Assuming that this is 88% of the total cooling, we would expect a total radiated flux from all species of ~0.97 ergs cm^{-2} s^{-1} sr^{-1}. This has to be compared with the kinetic energy inflow, which is $nmv^3/8\pi \sim 0.92$ ergs cm^{-2} s^{-1} sr^{-1}. The ratio of these two quantities yields $\Phi \sim 1.05$.

We are now in a position to compare the observed H_2O fluxes with the predicted ones. Table 11 of KN predicts the flux in a field of view 44″ in diameter for a shock with $\Phi \sim 3$. This field of view subtends a solid angle 0.34 times that of our ~75″ field. The H_2O abundances predicted using the gas-phase abundances from CMJS are only 0.41 times as high as the values

KN had assumed. These three effects partially cancel each other, but we have to divide the values listed in Table 11 of KN by 2.5 in order to apply their results to our observations with a 75″ beam.

Column (6) of Table 1 lists the ratios of the observed fluxes to the adjusted KN predictions based on the CMJS abundances. Given the wide range of energies E at which the upper levels for the transitions lie, $300 \lesssim E \lesssim 800$ K, it is unlikely that the observed-to-predicted line ratios would accidentally happen to fall into the narrow range in column (6) for all but one of the eight lines observed. Our abundance estimate assumes that the water line emission originates entirely in the shocked gas component and not in a lower temperature region. This is confirmed both by the line-strength ratios and by the observed line widths. Rigorous calculations, which we do not present here, confirm that the predicted H_2O fluxes scale almost linearly with H_2O abundance, although the average value of the actual-to-predicted line flux in column (6) drops by about 6% and the inferred abundances correspondingly rise by ~6%. For the substantial uncertainties in our flux calibrations, in our estimate of Φ, and in the abundance estimates, this agreement is reasonable. The deviant 121.7 μm line flux may reflect the neglect of radiative pumping by dust continuum radiation in the KN model. Preliminary calculations show that pumping by the ambient radiation field of Werner et al. raises the flux in this one line and leaves the other transitions essentially unaffected. Disregarding the anomalous 121 μm flux, we see that the observed values are roughly 30% higher than the predicted values.

5. DISCUSSION

Molecular shocks are important not only for their intrinsic interest but also because current views assume that star formation may well be triggered by shock compression followed by rapid cooling. The cooling needs to be rapid in order to prevent a quasi-elastic bounce that would permit shock-compressed regions to rebound to their original dimensions. If a shocked region is able to radiate away a substantial fraction of its energy during the traversal time of the shock, it will remain compressed. Even if it is not sufficiently dense at this stage to enter protostellar collapse, it will be poised to contract further if subjected to subsequent shocks.

We can estimate the integrated water vapor line flux from Orion summed over all transitions and compare it with the power radiated away by H_2 and CO. To estimate the total water vapor emission, we can sum the flux both from lines that we have observed and from lines whose strengths we infer by applying the KN model. This leads us to deduce a total water vapor emission of ~0.11 ergs cm^{-2} s^{-1} sr^{-1} normalized to a 75″ diameter solid angle. The beam-averaged CO flux from the region is ~0.13 ergs cm^{-2} s^{-1} sr^{-1}, obtained from the observational data cited in Stacey et al. (1983) and normalized to an assumed beam size of 60″—slightly smaller than the beam size used for our H_2O observations. This value, however, could drop by ~35% if the shocked region subtended a substantially smaller solid angle than our 75″ beam. The H_2O cooling and CO cooling of the shocked region are therefore comparable, but both are an order of magnitude lower than the total H_2 emission.

6. CONCLUSIONS

We have observed water vapor emission from the shocked region in Orion and find that the detected flux is consistent with a model proposed by KN, which inferred a shock velocity of ~37 km s^{-1} and a preshock H_2 density of ~10^5 cm^{-3}. However, the model can be correct only if we assume a water vapor abundance $n(H_2O)/n(H_2) \sim 5 \times 10^{-4}$ and a corresponding interstellar gas-phase oxygen abundance $n(O)/n(H) \sim 4 \times 10^{-4}$, in agreement with values cited by CMJS, in place of a substantially higher solar system abundance inferred from Pollack et al. (1994). Water vapor cooling in the shock is comparable to CO cooling but amounts to only ~10% of the total cooling provided by molecular hydrogen emission. Nevertheless, the KN model shows that H_2O and CO should dominate in that portion of the postshock region where temperatures are $\lesssim$800 K and neither vibrational nor rotational radiative cooling of H_2 is appreciable.

We wish to thank Steven Lord at IPAC and members of the LWS consortium in the UK for their advice on LWS data-reduction techniques. We also thank members of the help desk at VILSPA for their support. Michael Werner, the Letter's referee, made a number of clearly helpful comments. M. H. is pleased to acknowledge NASA grant NAG5-3347 to Cornell University; D. A. N has been supported by NASA grant NAG5-3316. G. J. M. would like to cite support through NASA LTSA grant NAG5-3542 and contract NAS5-30702, and M. J. K. is pleased to acknowledge support from NASA RTOP 344-04-10-02 and RTOP 864-03-08-90.

REFERENCES

Beck, S. C. 1984, ApJ, 281, 205
Beckwith, S., Persson, S. E., Neugebauer, G., & Becklin, E. E. 1978, ApJ, 223, 464
Cardelli, J. A., Meyer, D. M., Jura, M., & Savage, B. D. 1996, ApJ, 467, 334 (CMJS)
Cernicharo, J., Gonzáles-Alfonso, E., Alcolea, J., Bachiller, R., & John, D. 1994, ApJ, 432, L59
Chernoff, D. F., Hollenbach, D. J., & McKee, C. F. 1982, ApJ, 259, L97
Clegg, P. E., et al. 1996, A&A, 315, L36
Draine, B. T. 1980, ApJ, 241, 1021
Draine, B. T., & Roberge, W. G. 1982, ApJ, 259, L91
Elitzur, M., & de Jong, T. 1973, A&A, 67, 323
Elitzur, M., & Watson, W. D. 1978, A&A, 70, 443
Kaufman, M. J. 1995, Ph.D. thesis, Johns Hopkins Univ.
Kaufman, M. J., & Neufeld, D. A. 1996, ApJ, 456, 611 (KN)
Kessler, M. F., et al. 1996, A&A, 315, L27
Kwan, J., & Scoville, N. 1976, ApJ, 210, L39
Melnick, G. J., Stacey, G. J., Genzel, R., Lugten, J. B., & Poglitch, A. 1990, ApJ, 348, 161
Neufeld, D. A., & Melnick, G. J. 1987, ApJ, 332, 266
Pollack, J. B., Hollenbach, D., Beckwith, S., Simonelli, D. P., Roush, T., & Fong, W. 1994, ApJ, 421, 615
Stacey, G. J., Kurtz, N. T., Smyers, S. D., & Harwit, M. 1983, MNRAS, 202, 25P
Sugai, H., et al. 1994, ApJ, 420, 746
Viscuso, P. J., Stacey, G. J., Fuller, C. E., Kurtz, N. T., & Harwit, M. 1985, ApJ, 296, 142
Watson, D. M. 1982, Ph.D. thesis, Univ. California, Berkeley
Watson, D. M., Genzel, R., Townes, C. H., & Storey, J. W. V. 1985, ApJ, 298, 316
Watson, D. M., Storey, J. W. V., Townes, C. H., Haller, E. E., & Hansen, W. L. 1980, ApJ, 239, L129
Werner, M. W., Gatley, I., Harper, D. A., Becklin, E. E., Loewenstein, R. F., Telesco, C. M., & Thronson, H. A. 1976, ApJ, 204, 420
Zmuidzinas, J., Blake, G. A., Carlstrom, J., Keene, J., Miller, D., Schilke, P., & Ugras, N. G. 1995, in ASP Conf. Ser. 73, Airborne Astronomy Symp. on the Galactic Ecosystem: From Gas to Stars to Dust, ed. M. R. Haas, J. A. Davidson, & E. F. Erickson (San Francisco: ASP), 33